Journal of Materials Chemistry

Cite this: J. Mater. Chem., 2011, 21, 1880

www.rsc.org/materials

PAPER

Rapid direct growth of Li–Al layered double hydroxide (LDH) film on glass, silicon wafer and carbon cloth and characterization of LDH film on substrates

Zhi-Lun Hsieh, Meng-Chang Lin and Jun-Yen Uan*

Received 23rd August 2010, Accepted 1st November 2010
DOI: 10.1039/c0jm02779k

This work presents a novel method for directly growing highly oriented Li–Al LDH films on substrates such as glass, Si wafer and carbon cloth in an aqueous alkaline Al^{3+}- and Li^{+}-containing solution. The substrate samples were each hanged and then respectively immersed in the solutions at 5–35 °C for 20 min or less than 6 h to form the LDH films. The Li–Al LDH film comprised of extra-high-density Li–Al LDH platelets, each standing almost perpendicularly on the surface of the substrate. The LDH film that was fabricated at 5 °C (~1.4 μm thick) exhibits good UV shielding (with only 9.7% UV transparency) and a maximum of 56% transparency to visible light. A more rapid method (only 20 min needed) can be utilized to develop a Li–Al LDH film to cover both hydrophobic and hydrophilic carbon cloth surfaces. Despite the modification of these surfaces, the Li–Al LDH film on carbon cloths retained or enhanced their original surface properties (including hydrophobicity or hydrophilicity). The LDH film thickness increased with immersion time and/or solution temperature. The thickness reached a plateau during LDH formation. CO_2 in the atmosphere dissolved in the alkaline Al^{3+}- and Li^{+}-containing solution, yielding CO_3^{2-} ions for Li–Al LDH formation. The heterogeneous nucleation and growth of each LDH platelet on the substrate surface finally produced an LDH film.

Introduction

Layered double hydroxides (LDHs) consist of positively charged layers, with anions and water molecules intercalated in the interlayer region. The chemical compositions of LDHs are represented by the general formula $[M^{z+}_{1-x}M^{3+}_{x}(OH)_2]^{A+}$ $[X^{m-}]_{A/m}\cdot nH_2O$ where M^{z+} and M^{3+} represent metallic cations, respectively, and X^{m-} represents the interlayer anion. For $z = 2$, M^{2+} may be Ca^{2+}, Mg^{2+}, Zn^{2+}, Ni^{2+}, Mn^{2+}, Co^{2+}, Fe^{2+} or Cu^{2+}, and M^{3+} can be Al^{3+}, Cr^{3+}, Mn^{3+}, Fe^{3+}, Ga^{3+}, Co^{3+}, or Ni^{3+}; X^{m-} can be SO_4^{2-}, CO_3^{2-}, Cl^-, OH^-, NO_3^-, PO_4^- or I^-.[1,2] LDHs have also been prepared with $z = 1$. A unique compound in the LDHs that contains monovalent and trivalent matrix cations is $[Li^{+}_{1-x}Al^{3+}_{x}(OH)_2]^{(2x-1)+}$ $(X^{m-}_{(2x-1)/m})\cdot nH_2O$ (X^{m-} = CO_3^{2-}, Cl^-, SO_4^{2-} or $Fe(CN)_6^{4-})^{2-6}$ (Li–Al LDH, hereafter). Two main methods that have been proposed to synthesize Li–Al LDH powder, is as follows. They are co-precipitation[2,3,6] and intercalation.[4,5] The authors' earlier investigation[7] explored a novel method that was based on a metal salt-free system for synthesizing a Li–Al–CO_3 LDH by adding powdered AlLi intermetallic compound (IMC) to a stirred water bath at ambient temperature in the ambient atmosphere. The AlLi powder was hydrolyzed strongly, yielding an alkaline Al^{3+}- and Li^{+}-containing aqueous solution of pH 12.3.[7] Dissolution of the CO_2 gas from the ambient atmosphere in the stirred alkaline solution caused the anion, CO_3^{2-}, in the solution to form Li–Al–CO_3 LDH.[7] The results of the authors' earlier work[7] implies that the formation of Li–Al–CO_3 LDH depends on nucleation and growth in the solution. One of the main goals of this study is to place various inert substrates in the Al^{3+}- and Li^{+}-containing aqueous solution to investigate the heterogeneous nucleation and growth of highly-oriented Li–Al–CO_3 LDH on the substrates.

Because of the diversity of the chemical compositions of brucite-like host layers and interlayer anions, several LDHs with a wide range of technological applications have been fabricated. They include catalysts,[8–11] absorbents,[12–14] anion exchangers,[15] sensors,[16] bio-sensors,[17] and biomolecular carriers.[18] Recently, Corma *et al.*[19] showed that calcined Li–Al LDHs powders can catalyze the glycerolysis of fatty acid methyl esters to monoglycerides (the reverse of biodiesel synthesis). An uncalcined Li–Al LDH, $[Al_2Li(OH)_6]OH\cdot nH_2O$ powder has also recently been found to be active in the transesterification of 5-carboxyfluorescein diacetate with 1-butanol.[20] Shumaker *et al.*[21,22] found that calcined $[Al_2Li(OH)_6](CO_3)_{0.5}\cdot nH_2O$ powder is a highly effective catalyst for the transesterification of soybean oil with methanol. However, according to some investigations,[23–35] powdered catalysts are not practical for commercial use because they are associated with a large pressure drop,[23–29] difficult to separate from the reaction products,[25,27,30–32] tending to aggregate,[31–33] and having a low

Department of Materials Science and Engineering, National Chung Hsing University, 250 kuo – kuang Rd., Taichung, 402, Taiwan, ROC. E-mail: jyuan@dragon.nchu.edu.tw; Fax: +886-4-22857017; Tel: +886-4-22854913

thermal conductivity.[26,28] Thus, all of which properties make their application difficult to scale-up.[23,27,30] Therefore, the feasibility of fixing LDHs on nanofibers[36] and monolithic substrates[37,38,40–51] and of preparing macro-scale LDH spheres[23,38,39] has attracted a great interest in LDH research. Moreover, Indira and Kamath,[52] Scavetta *et al.*[53] and Yarger *et al.*[54] have also performed studies to electrochemically synthesize LDH thin films on Pt or Au substrate. Sasaki and co-workers[40] achieved the layer-by-layer self-assembly of the LDH nanosheets and anionic polymers to produce multilayer composite films on Si wafer and on glass slide. Lee *et al.*[41] immobilized the synthesized Mg–Al LDH nanocrystals on a Si wafer by immersing the wafer, facing upwards, in the colloidal solution (Mg–Al LDH powder + organic solvent (*e.g.*, toluene)). According to Okamoto *et al.*,[42] a mixture of Mg–Al LDH crystals and deionized water was cast onto a glass substrate, and then dried to form a Mg–Al LDH thin film. The procedures to yield the films mentioned above are proceeded by the face-to-face stacking of the LDH platelets and the resulting structures have 2D sheet-like structure.[41,42] Guo *et al.*[37] suggested that the adhesion between the LDH crystallites produced by the above deposition method will be much weaker than in the films fabricated by *in situ* growth. Lu *et al.*[43] developed an *in situ*-grown Mg–Al LDH film on an anodic aluminium oxide (AAO)/aluminium substrate by suspending the AAO/aluminium substrate in a mixed solution ($Mg(NO_3)_2$ + urea + deionized water) at 70 °C. The Mg–Al LDH layer formed on the AAO over a long period of 168 h.[43] Chen *et al.*[44] focused on an *in situ* way to develop Ni–Al LDH film and Zn–Al LDH film on a porous anodic alumina/aluminium (PAO/Al) substrate by suspending vertically the PAO/Al substrate in a special solution at 75 °C for 36 h. Liu *et al.*[45] observed that a ZnO/Zn–Al LDH film can be grown on the surface of an Al substrate by dipping an Al substrate in an Zn^{2+}-containing solution ($Zn(CH_3COO)_2$ + $NH_3 \cdot H_2O$) at 60 °C for 24 h. Alternatively, Zn–Al LDH film and Cu–Al LDH film were grown on Zn foil and Cu foil, respectively, by suspending a Zn (or Cu) foil and an Al foil into an alkaline solution at room temperature.[46] As long as three days were necessary to obtain the LDH film on the bivalent metal substrate.[46] Guo *et al.*[47] developed Mg–Al LDH film *in situ* by urea hydrolysis on a pure aluminium substrate by placing the metal substrate vertically in a mixed solution ($Mg(NO_3)_2 \cdot 6H_2O$ + $(NH_2)_2CO$ + deionized water) at 90 °C for 6 h. According to the above methods, one of the metal cations in a fabricated LDH originates in the metal substrate, because of alkali etching. Uan *et al.*[38] presented a novel scheme for developing a highly-oriented Mg–Al LDH on the surface of an Mg–Al–Zn alloy plate by simply dipping the sample in aqueous HCO_3^-/CO_3^{2-}. According to Uan *et al.*,[38] the substrate surface corrodes in the solution, and thus providing both Mg^{2+} and Al^{3+} to form Mg–Al LDH film on the Mg alloy surface. Although the cited studies have made progress in the direct growth of LDH coatings on substrates, qualified substrates must be able to react with the solution to provide cations to form the LDH at the substrate surface. Moreover, it takes a long time (6 h–168 h) to yield the *in situ*-grown LDH films on substrates. A question is thus raised concerning whether a highly-oriented LDH film can grow directly on an inert substrate in a relatively short time. Such substrate's surface almost does not react with alkaline cation-containing solution, and so provide no cations to promote the coating of LDH on the substrate. Duan and co-workers[48–50] have made progress on *in situ* growth of LDH on polystyrene sheets,[48] glass,[49] paper,[50] cloth[50] and sponge.[50] According to their studies,[48–50] the substrate samples do not provide cations for the LDH formation. Nevertheless, for instance, the surface of the polystyrene firstly has to be sulfonated in 98% sulfuric acid for as long as 72 h.[48] It was followed by placing the sulfonated polystyrene in the aqueous solution containing Mg^{2+}, Al^{3+} and urea.[48] Li *et al.*[51] prepared Ni–Al LDH film on Ti substrate by a coprecipitation method. Again, no cations originate in the Ti substrate to form the Ni–Al LDH film.[51] However, it takes 24 h at 95 °C to fabricate the LDH film.[49] Typically, low fabrication temperature and rapid synthesis are two of the important issues in connection with producing LDH film. Moreover, Duan and co-workers[37] reported that there is considerable scope for the development of additional new preparation methods, which will extend the range of new LDH films. Thus, this investigation addresses a metal salt-free method for *in situ*-grown Li–Al LDH film on various inert substrates at 5–35 °C for a relatively short time. Experimentally, high-density *in situ*-grown LDH platelets were formed on substrates such that each stood almost perpendicularly to the substrate surface. The thickness of the LDH film that grew on a glass substrate as a function of time was measured. For instance, ~1 μm thick of uniform Li–Al LDH film would directly grow on a glass substrate after 1 h treatment. The crystal structure, chemical composition, optical transmittance and hydrophobicity of the Li–Al LDH film were characterized.

Experimental procedures

Preparation of Al^{3+}- and Li^+-containing solution

AlLi IMC is the key material that is used herein to synthesize Li–Al LDH. The formula of the intermetallic compound is AlLi

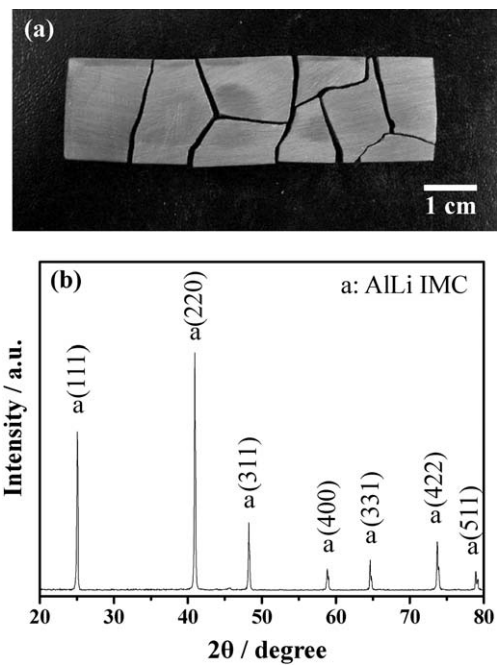

Fig. 1 (a) Bulk AlLi IMC, showing the brittle nature of the IMC; (b) XRD pattern of the AlLi IMC.

(JCPDS 3-1215). The authors' earlier study[7] detailed the procedures for preparing the AlLi IMC. Fig. 1(a) presents the AlLi IMC prepared in this investigation, revealing the brittleness of the IMC. The crystal structure of the AlLi IMC sample was verified by X-ray diffraction (Fig. 1(b), JCPDS 3-1215). Since the AlLi IMC is brittle, the AlLi IMC powder was prepared by breaking and grinding the IMC compound in a mortar. AlLi IMC exhibits high activity in water and so hydrolyzed therein.[7] The AlLi powder was added to 100 ml DI water under continuous stirring for 5 min at room temperature in the ambient atmosphere. H_2 was generated, bubbling for about 10 s during the hydrolysis of the AlLi IMC powder in the DI water. The reaction solution was filtered through filter paper (No.5A; Advantec). The pH of the filtered aqueous solution was about 12.3. The solution was examined using ICP (ICP-AES, ULTIMA 2000, Horiba Jobin Yvon) to determine the concentrations of Al^{3+} and Li^+. When 0.2 g AlLi IMC powder was used, the Al^{3+} and Li^+ concentrations in the solution were 370 ± 26 ppm and 291 ± 73 ppm, respectively. Hereafter, this solution was denoted as Solu_A. When 0.4 g AlLi IMC powder was used, the filtered solution contained final concentrations of Al^{3+} 1070 ± 69 ppm and Li^+ 594 ± 9 ppm. This solution was denoted as Solu_B.

Direct growth of Li–Al LDH on alkaline earth boro-aluminosilicate (AEBA) glass and Si wafer

Alkaline earth boro-aluminosilicate (AEBA) glass (Corning® EagleXG™) of size 10 × 10 × 0.64 mm^3 and a Si (100) wafer sample of size 10 × 10 × 0.80 mm^3 were used in this study. Each Si wafer was cleaned ultrasonically in ethyl alcohol, and then dried in air. Each AEBA glass was cleaned ultrasonically in NaOH solution (pH∼12), washed in DI water, and then dried in air. The AEBA glass and Si wafer were each immersed into Solu_A for 1 h, 3 h and 6 h in the ambient atmosphere. The resulting samples were dried under vacuum at room temperature. The surface microstructures of the treated samples were observed using a field-emission scanning electron microscope (SEM, JEOL JSM-6700F). The crystallographic structures that developed in the sample were then determined by glancing angle X-ray diffraction (GAXRD) with a glancing angle of 1° using Cu Kα1 (1.5406 Å) radiation. The FTIR spectrum of the treated samples was determined using a DIGILAB FTX3500 instrument at wavenumbers from 400 to 4000 cm^{-1}.

To determine the effect of temperature on the thickness of the Li–Al LDH film on an inert substrate, AEBA glass was immersed in Solu_A at various temperatures (5, 16, 28 and 35 °C (±1 °C)) for various periods. Highly pure N_2 gas was bubbled through the solution as it was heated or cooled to the experimental temperature. The bubbling of N_2 prevented the dissolution of CO_2 during the heating or cooling process. The bubbling ceased when the LDH coating experiments were conducted. After cleaning the glass samples by the same method mentioned above, each was hung and placed vertically in a beaker that contained 45 ml of Solu_A at a known temperature for specified time in ambient atmosphere. The resulting samples were dried at room temperature.

The thickness of the Li–Al LDH film on AEBA glass was measured by the α-step method. FTIR spectra of the treated samples were obtained using a DIGILAB FTX3500 instrument at wavenumbers from 400 to 4000 cm^{-1} at room temperature. The optical transmittance and absorption spectra of the Li–Al LDH film on AEBA glass were measured at wavelengths 260–900 nm using a Hitachi U-3010 spectrophotometer. The contact angle of the water on the surface was measured using a contact angle analyzer (FTA-2000, First Angstrom Co.).

Direct growth of Li–Al LDH on carbon cloth

Commercial hydrophobic carbon cloth and hydrophilic carbon cloth were both used herein. Each sample had an area of 15 × 15 mm^2. Carbonated water (aqueous HCO_3^-/CO_3^{2-} solution) was firstly prepared at room temperature by bubbling CO_2 gas through 100 ml of DI water. The authors' earlier studies[38,55,56] have described in detail the procedures for preparing the carbonated water. The hydrophobic carbon cloth and hydrophilic carbon cloth were immersed in the carbonated water for 20 min. After immersion for 20 min in the carbonic acid, the two carbon cloth samples were removed and placed in another beaker that contained 95 ml of Solu_B. The period of immersion was 20 min. The treated samples were dried *in vacuo* at room temperature. The surface microstructures of the treated samples were observed using a field-emission SEM. The LDH material on the carbon cloth was studied by GAXRD at a glancing angle of 1° using Cu Kα1 (1.5406 Å) radiation. The contact angle of water on the carbon cloth surface was measured using a contact angle analyzer (FTA-2000, First Angstrom Co.).

Results and discussion

Fig. 2 presents each of the X-ray patterns from the pieces of AEBA glass and Si wafer that were treated in Solu_A at room

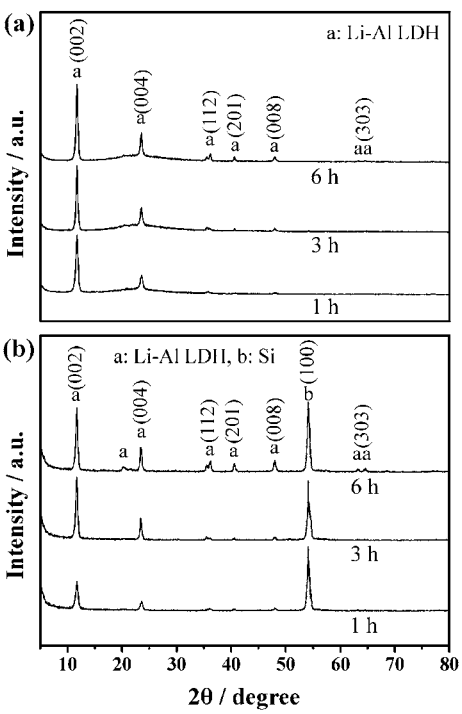

Fig. 2 GAXRD patterns of the Li–Al LDH obtained with different immersion time at room temperature (∼28 °C) on: (a) AEBA glass (b) Si wafer.

temperature for various intervals. The GAXRD patterns included intensity peaks of Li–Al-CO_3 LDH (JCPDS 42-729). The X-ray peaks were indexed as belonging to a hexagonal crystal system (JCPDS 42-729). Moreover, according to the experimental results and calculations by Drewien *et al.*[57] and the author's earlier work,[7] the crystal structure of Li–Al–CO_3 LDH was also found to be hexagonal. As revealed by the GAXRD patterns in Fig. 2(a), the glass sample that had been immersed for 1 h yielded X-ray peaks of Li–Al-CO_3 LDH. The X-ray peaks of the Li–Al-CO_3 LDH became more intense as the immersion time was increased to 3 h and then to 6 h (Fig. 2(a)). Fig. 2(b) displays the GAXRD pattern of each of the Li–Al-CO_3 LDH coatings on the Si (100) wafers that were treated in the aqueous solution at room temperature for different times. The sample that had been immersed for 1 h yielded relatively weak X-ray peaks of Li–Al-CO_3 LDH. Strong X-ray peaks of the LDH could be obtained as extending the immersion time to 6 h. Fig. 3(a) presents the FTIR spectrum of the LDH platelets on the surface of the AEBA glass. Fig. 3(b) presents the FTIR spectrum of the LDH platelets on the surface of the Si wafer. Fig. 3(a) and (b) yielded a similar spectrum. The broad transmission band at around 3470 cm^{-1} (Fig. 3(a), (b)) corresponds to the stretching vibrations of the H-bonds of the OH group in the hydroxide layer.[58,59] A shoulder band at about 3080 cm^{-1} (Fig. 3(a), (b)) suggests the presence of water molecules that are hydrogen-bonded to the carbonate ions in the interlayer.[58,59] The transmission band at ~1375 cm^{-1} is the CO_3^{2-} absorption band.[58,59] The transmission band at about 1000 cm^{-1} (Fig. 3(a), (b)) is associated with the vibrations of the hydroxyl groups that are coordinated with the cations (Al^{3+} and Li^+, herein) in the octahedral $Al(OH)_3$ layers.[58,59] In the low-frequency region, the three bands around 757, 713 and 530 cm^{-1} are related to the Al–O stretching vibrations.[58,59] Hence, the

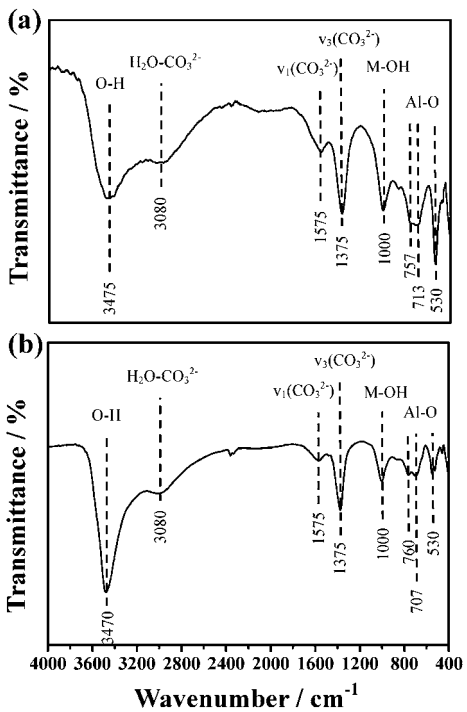

Fig. 3 FTIR spectra of the Li–Al LDH formed on (a) AEBA glass, (b) Si wafer.

Table 1 Li and Al contents of the LDH grown on AEBA glass, by ICP-AES analysis

	Composition (wt.%)		
Sample	Li	Al	Al/Li (atomic ratio)
Li–Al LDHs on AEBA glass	2.49	19.40	2.00

FTIR spectra of the LDH platelets on the surface of the AEBA glass and the Si wafer include the main bands of Li–Al–CO_3 LDH. Table 1 shows the quantitative ICP-AES analysis of the Li and Al contents of the Li–Al LDH on the AEBA glass. According to this table, the Al/Li atomic ratio of the LDH sample was 2.00, close to that of $Li_2Al_4(CO_3)(OH)_{12}\cdot mH_2O$.

Fig. 4 displays the surface microstructure and the cross-sectional view of the LDH layer on AEBA glass. As shown in Fig. 4(a), the LDH platelets stand upward and adjacent to each other to form a film that covered the glass. Immersion for 3 h or 6 h thickened the layer of oriented LDH platelets on the AEBA glass (as presented in Fig. 4(b) and (c)). The same procedure also yielded a thick layer of *in situ*-grown LDH on the Si wafer, as presented in Fig. 5(a) to (c). The LDH platelets grew directly from the surface of the Si wafer, with each of the LDH platelets standing almost perpendicular to the surface of the Si wafer. According to several SEM examinations on very initial growing stage at substrate surface and the uniform growing stages (Fig. 4 and 5), we confirm that Li–Al LDH grew directly on the AEBA

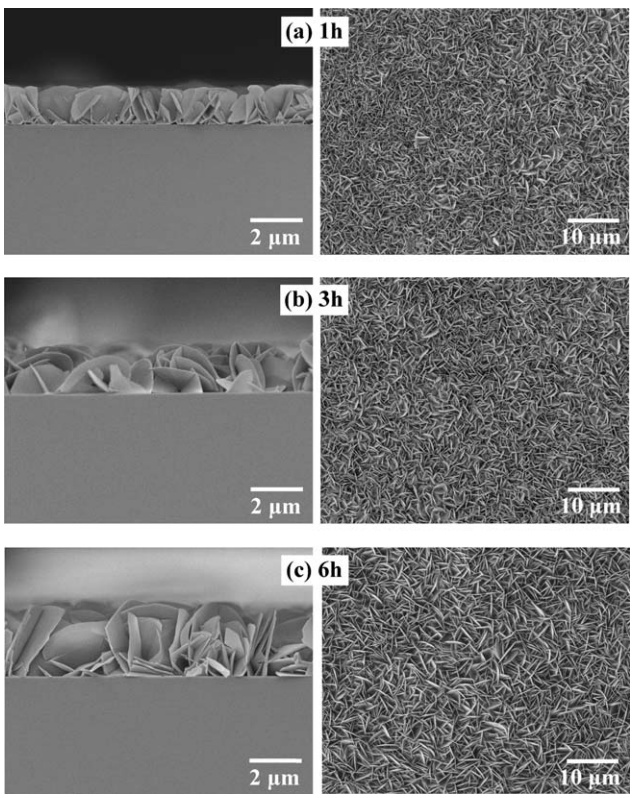

Fig. 4 SEM cross-sectional microstructures and surface morphologies of LDH thin films grown on AEBA glass at room temperature (~28 °C) with immersion time: (a) 1 h; (b) 3 h; (c) 6 h.

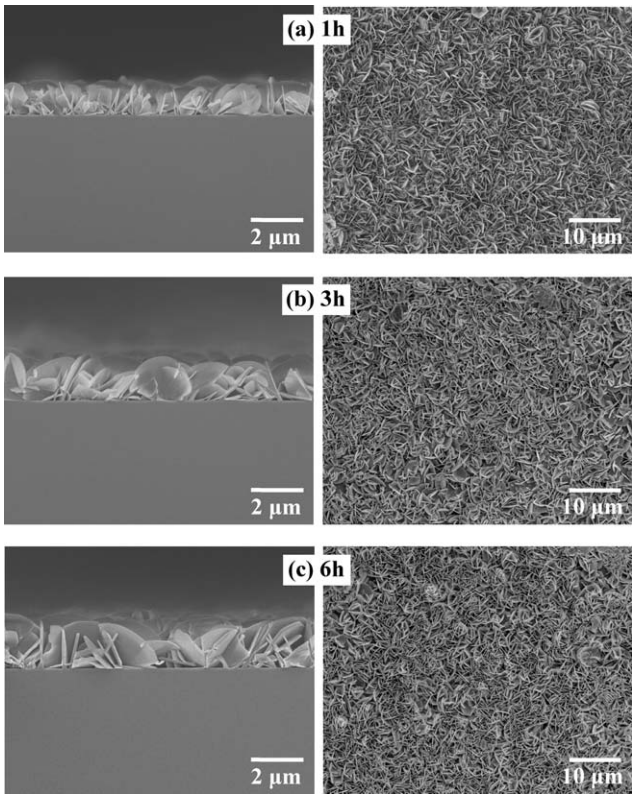

Fig. 5 SEM cross-sectional microstructures and surface morphologies of LDH thin films grown on Si wafer at room temperature (~28 °C) with immersion time: (a) 1 h; (b) 3 h; (c) 6 h.

glass and Si wafer by this study's immersion treatment in the aqueous solution (pH~12.3) herein.

Fig. 6 plots the relationship between the thickness of the LDH film that grew on AEBA glass and the immersion time. The temperatures in Fig. 6 were temperatures of Solu_A. As shown in Fig. 6, the growth rate of the LDH film thickness exhibited two distinct regimes as the immersion time varied. In regime I at each temperature, the LDH film grows linearly with time on the AEBA glass substrate. Regime II is plateau-like, such that the thickness of the LDH film at each temperature was static. The static thickness increased with temperature. Fig. 7 presents the surface microstructures of the glass samples following LDH

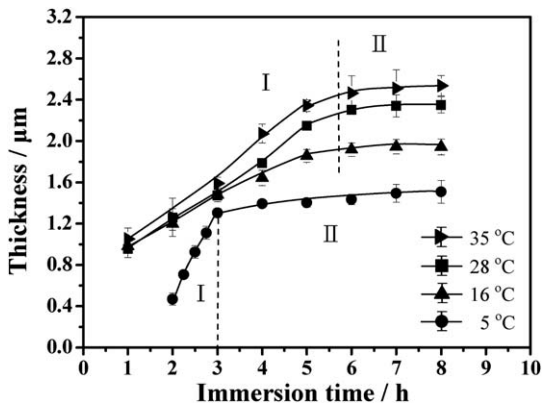

Fig. 6 LDH film thickness on AEBA glass as a function of immersion time (LDH growth time) at different formation temperatures.

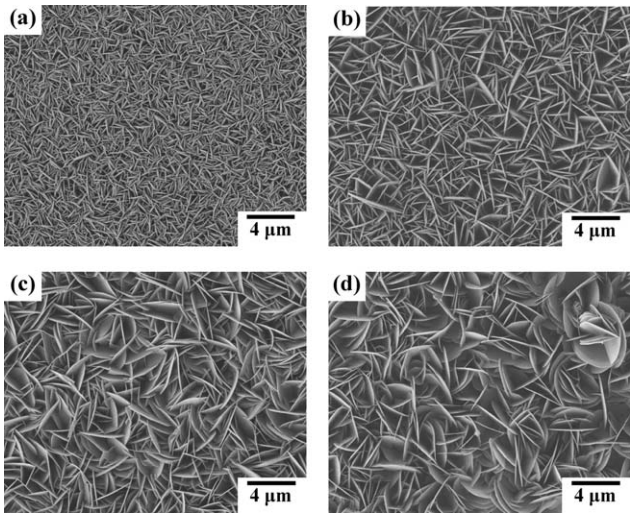

Fig. 7 SEM surface morphologies of the LDH thin films grown on AEBA glass at different temperatures (a) 5 °C; (b) 16 °C; (c) 28 °C; (d) 35 °C after 6 h immersion.

formation at various temperatures. As shown above in Fig. 6, at a higher temperature, a thicker Li–Al LDH film formed on the glass. Similarly, comparing each of the microstructures in Fig. 7 reveals that the size of the LDH platelets that formed at 5 °C (Fig. 7(a)) was the smallest. Larger LDH platelets were formed when the formation temperature was increased to 16 °C (Fig. 7(b)). The platelets on the samples on which the platelets were formed at 28 °C (Fig. 7(c)) and 35 °C (Fig. 7(d)) were slightly larger than those that formed at 16 °C. As shown above in Fig. 4 and 5, an Li–Al LDH thin film formed on AEBA glass and Si wafer not with parallel face-to-face stacking of LDH platelets, but such that each LDH platelet in the LDH film stood upright. Thus, the increasing thickness of the LDH film represented that each LDH platelet was growing higher and wider.

The Li–Al LDH coating may change the surface properties of the glass. Fig. 8 displays the shape of the water droplet on the

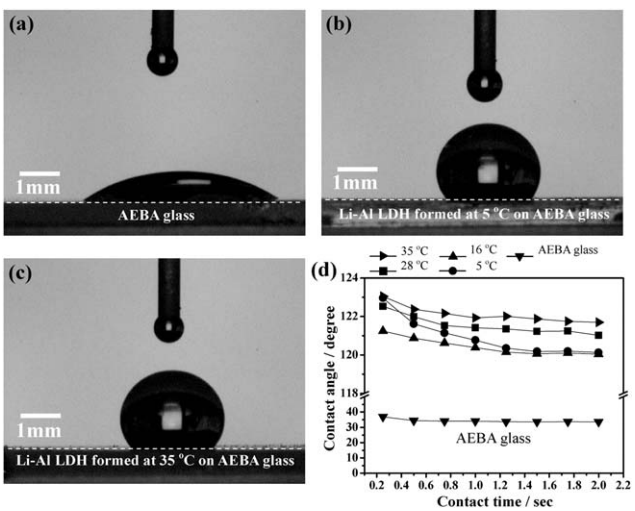

Fig. 8 Optical micrographs of the static water drop on (a) AEBA glass, and on the glasses with the LDH coatings formed at (b) 5 °C; (c) 35 °C; (d) water contact angles as a function of contact time on AEBA glass and the glasses with LDH coatings formed at different temperatures.

AEBA glass with and without an Li–Al LDH coating. As shown in Fig. 8(a), the droplet on the AEBA glass became flat, with a constant contact angle of ~33° as a function of the contact time (see the data in Fig. 8(d)). Hence, the AEBA glass surface was hydrophilic. When the surface was coated with Li–Al LDH, as displayed in Fig. 8(b) and 8(c), the shape of the water droplet on the Li–Al LDH film showed relatively high contact angle. Fig. 8(d) plots the contact angles of water on the Li–Al LDH-coated samples. The data verify that the Li–Al LDH coating was strongly hydrophobic.

Fig. 9 (a) and (b) present the transmittance and absorbance spectra of Li–Al LDH films that grew on AEBA glass at 5 °C and 28 °C for 6 h. The spectra in Fig. 9 can be divided by wavelength into three regions—UV (200–400 nm), visible light (400–780 nm) and near-infrared light (larger than 780 nm). The LDH-coated glass sample, on the surface of which the LDH film formed in 6 h at 5 °C, was denoted as 5 °C–LDH–AEBA. Similarly, the term 28 °C–LDH–AEBA can be found below. Although the transmittance and absorption spectra of the bare AEBA glass are not shown here, almost 100% transparency to UV, visible and near-infrared light was experimentally confirmed. As shown in Fig. 9(a), the transmittance of 28 °C–LDH–AEBA was less than 1% in the UV region, and reached a maximum of 9.4% in the visible region. Moreover, the 28 °C–LDH–AEBA had a relatively high transmittance in the near-infrared region. The 5 °C–LDH–AEBA sample had smaller LDH platelets and a thinner LDH film than the 28 °C–LDH–AEBA sample. As shown in Fig. 9(a), 5 °C LDH–AEBA has a transparency to UV light of less than 10%, and a maximum transparency to visible light of 56%. As presented in Fig. 9(b), the absorption capacity of both samples was low (less than 2.2%) over the whole range of wavelengths, suggesting that the LDH platelets reflected most of the light. In recent studies,[60–63] Mg–Al LDH and Zn–Al LDH have been used as starting materials in the preparation of new UV-shielding products or sunscreen products, in which organic UV absorbents are intercalated into LDH hosts. The entrapping of organic UV absorbents between LDH lamellae can protect the organic absorbents against thermal degradation[62] or prevent direct contact between them and skin.[61] Li *et al.*[60] and He *et al.*[61] prepared thin films (both ~1.25 μm thick) made of LDH powders (with or without the intercalated UV absorbents). Li *et al.*[60] found that a thin film of Zn–Al LDH that is intercalated with UV absorbent has a maximum UV transparency of ~20%, whereas 60% to 80% of UV passes through a pure Zn–Al LDH film. He *et al.*[61] found similarly that a thin film of pure Zn–Al LDH exhibits poor UV shielding property. In the present study, no organic UV absorbent was used to prepare an LDH film (5 °C–LDH–AEBA) with relatively strong UV shielding and moderate transmittance of visible light.

Fig. 10 presents the X-ray patterns of the original hydrophobic and hydrophilic carbon cloths and those that were treated in Solu_B at room temperature for 20 min. The X-ray patterns in Fig. 10(a) include the intense peak of polytetrafluoroethylene (PTFE). The PTFE was coated on the carbon cloth to increase the hydrophobicity of the carbon cloth. According to the GAXRD results in Fig. 10(a), the pattern of the sample that had been immersed in Solu_B for 20 min yielded X-ray peaks of Li–Al LDH. PTFE remained on the carbon cloth after it was treated. Fig. 10(b) presents the GAXRD patterns of the hydrophilic carbon cloth and the cloth that was treated in Solu_B at room temperature for 20 min. The X-ray pattern of the latter

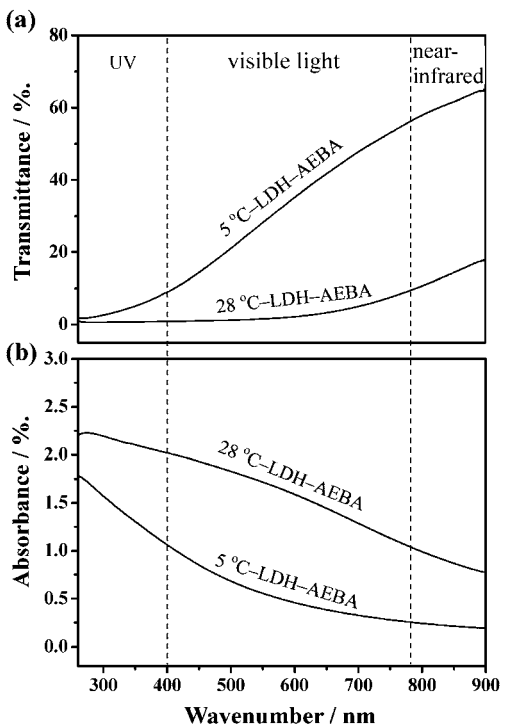

Fig. 9 UV-visible (a) transmittance spectra and (b) absorption spectra of the Li–Al LDH-coated AEBA glass at 5 °C and 28 °C.

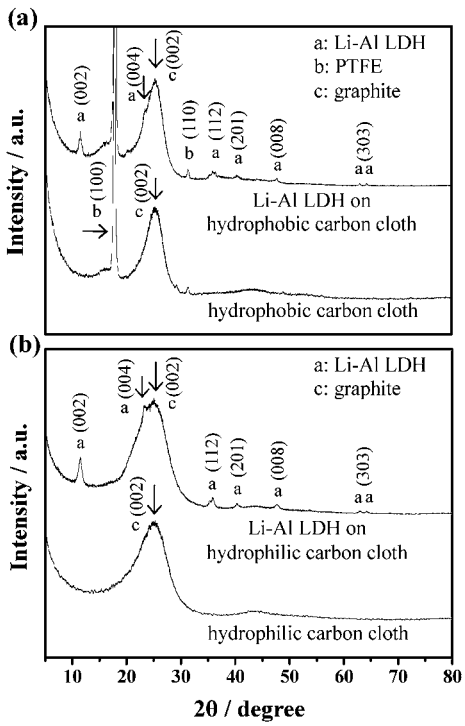

Fig. 10 X-Ray diffraction patterns of the carbon clothes with and without Li–Al LDH coating (a) hydrophobic carbon cloth, (b) hydrophilic carbon cloth after 20 min treatment at room temperature.

includes peaks of Li–Al LDH. Fig. 11(a) and (b) show the photographs of the surface microstructures on the hydrophobic carbon cloth before and after LDH coating treatment, respectively. As displayed in Fig. 11(a) (before LDH treatment), PTFE is present between some of the carbon fibres. Fig. 11(b) reveals several tiny nodules on the carbon fibres and between the fibres of the hydrophobic carbon cloth. The inset in Fig. 11(b) presents the microstructure on the fibre's surface at high magnification, revealing rosette-like Li–Al LDH aggregates. Fig. 12(a) displays the hydrophilic carbon cloth before LDH coating treatment, showing free space between each fibre. The microstructure, as shown in Fig. 12(b), and the inset in the figure present the surface microstructure of the hydrophilic carbon cloth. As presented, a high density of LDH platelets covered and stood perpendicular to the surface of the carbon fibres.

Fig. 13 and 14 present the shapes of the water droplets on the carbon cloths before and after they had been coated with a Li–Al LDH film. Fig. 13(a) plots the contact angle of water on the surface of the hydrophobic carbon cloth and on the surface of the LDH-coated hydrophobic carbon cloth against contact time. It reveals that the contact angle remained almost constant. The contact angle on the hydrophobic carbon cloth at a contact time of 2 s had slightly declined to 126.6°, while that on the LDH-coated hydrophobic cloth had slightly decreased to 121.4°. As shown in Fig. 13(b) and (c), the shape of the water droplet on the hydrophobic cloth was similar to the shape of the droplet on the LDH-coated cloth. Importantly, the hydrophobic cloth surface

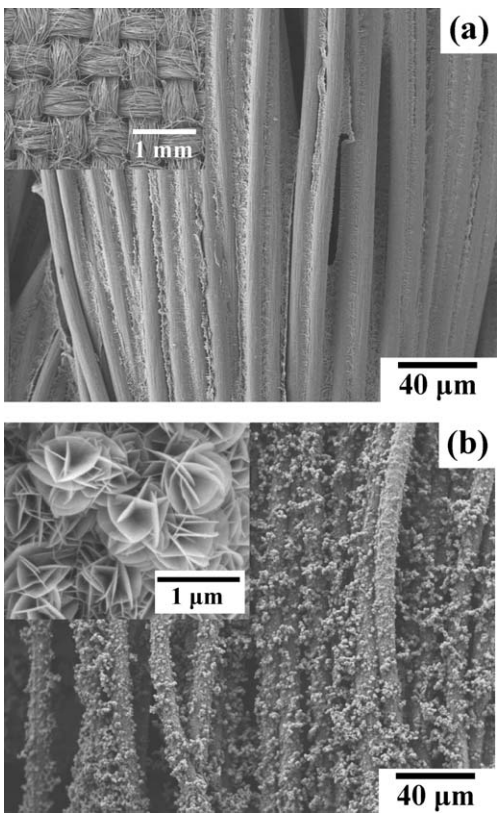

Fig. 11 SEM surface morphologies of (a) hydrophobic carbon cloth without LDH coating and (b) LDHs thin films grown on hydrophobic carbon cloth at room temperature after 20 min treatment.

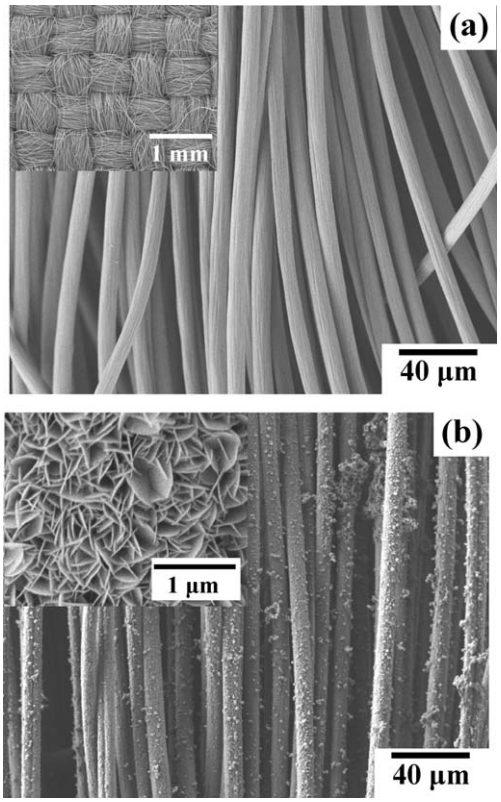

Fig. 12 SEM surface morphologies of (a) hydrophilic carbon cloth without LDH coating and (b) LDHs thin films grown on hydrophilic carbon cloth at room temperature after 20 min treatment.

that was covered with the LDH platelets retained good hydrophobicity. Fig. 14(a) plots the contact angle of water on the surface of the hydrophilic carbon cloth and on the LDH-coated hydrophilic carbon cloth *versus* contact time. The contact angle on the hydrophilic carbon cloth was ~78.8° at 0.25 s. Thereafter, as the contact time increased to 2 s, the contact angle fell slightly to ~68° (see Fig. 14(b) for the droplet shape). The contact angle of the LDH-coated hydrophilic carbon cloth was ~72.3° at 0.25 s, and declined remarkably to 0° at 0.75 s (see the data in Fig. 14(a)). Accordingly, the droplets on the LDH-coated hydrophilic carbon cloth, shown in Fig. 14(c), were flattened out, indicating that the hydrophilic cloth surface that was modified by the LDH film exhibited even greater hydrophilicity than the original cloth. As presented above in Fig. 8, the Li–Al LDH film was highly hydrophobic, raising the question of why the hydrophilic cloth surface that was modified by the LDH film could exhibit excellent hydrophilicity (Fig. 14). SEM micrograph from a LDH-coated hydrophilic carbon cloth, as illustrated in Fig. 15(a), shows a side view of the cloth. LDH coatings are observed on the fibres that are close to the surface of the hydrophilic carbon cloth surface (Fig. 15(b)). The fibres under the surface of the hydrophilic carbon cloth have no LDH coating (Fig. 15(c)). Therefore, the LDH-coated hydrophilic carbon cloth has hydrophobic fibres on its surface but contains hydrophilic fibres inside. Hence, when a water droplet falls on the carbon cloth, it is repelled by the surface fibres. The repulsion drives the water through the spaces between the fibres (whose spacing is as displayed in Fig. 12(a)) to the interior of this

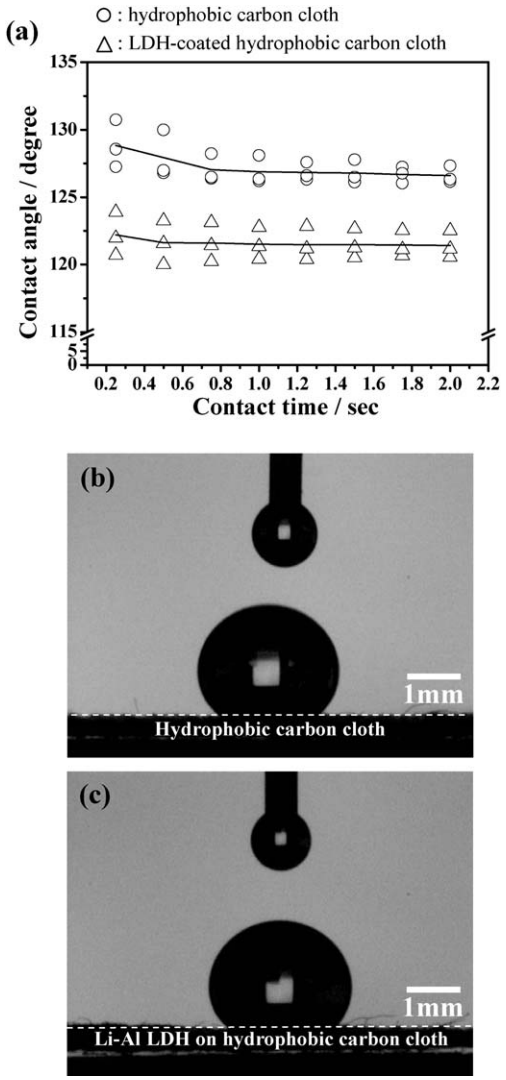

Fig. 13 (a) Water contact angles on the hydrophobic carbon clothes with and without LDH coating as a function of contact time; (b) and (c) optical micrographs of the water drops on hydrophobic carbon cloth at 2 s contact time (b), and on LDH-coated hydrophobic carbon cloth at 2 s contact time (c).

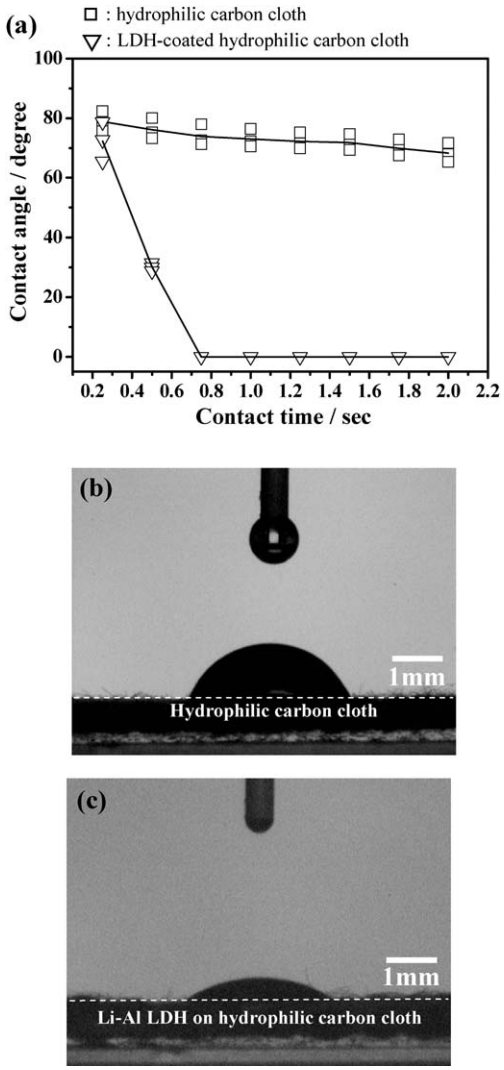

Fig. 14 (a) Water contact angles on the hydrophilic carbon clothes with and without LDH coating as a function of contact time; (b) and (c) optical micrographs of the water drops on hydrophilic carbon cloth at 2 s contact time (b), and on LDH-coated hydrophilic carbon cloth at 0.5 s contact time (c).

hydrophilic cloth, leading to the excellent hydrophilicity of a Li–Al LDH coated hydrophilic carbon cloth.

Conclusions

This study elucidates a metal salt-free method for directly growing a highly-oriented Li–Al–CO_3 LDH film on various inert substrates at temperatures 5–35 °C in an alkaline aqueous solution that contained Li and Al ions. The solution was prepared by simply adding AlLi IMC powder to DI water. Carbon dioxide in the ambient atmosphere dissolved in the alkaline solution, yielding CO_3^{2-}. The nucleation and growth of Li–Al–CO_3 LDH crystal on the substrate surface proceeded when the substrate was perpendicularly immersed into the Al^{3+}- and Li^{+}-containing solution for 20 min or less than 6 h. The period for the LDH film formation depends on the substrates employed and the LDH film thickness expected. The Li–Al–CO_3 LDH film herein comprised extra-high-density LDH platelets, each standing roughly perpendicular to the substrate surface. The LDH film thickness increased with the immersion time. Finally, the LDH film reached a constant thickness. The LDH film that was fabricated by this approach did not have to be washed in water because metal salts are not used in the formation of an LDH film. Li–Al LDH-coated glass exhibited excellent UV shielding capacity with a transparency to UV of less than 10%, with a maximum transparency to visible light of ~56%. The UV shielding characteristic of the LDH film herein did not depend on the use of organic UV absorbent. Extra-high-density Li–Al LDH platelets were formed on the carbon fibre surface of a hydrophobic or hydrophilic carbon cloth. Although the surface of a carbon cloth was thereby modified to have a high surface area, their original property (such as hydrophobicity or hydrophilicity) was unaltered or enhanced. The proposed method represents a new scheme for

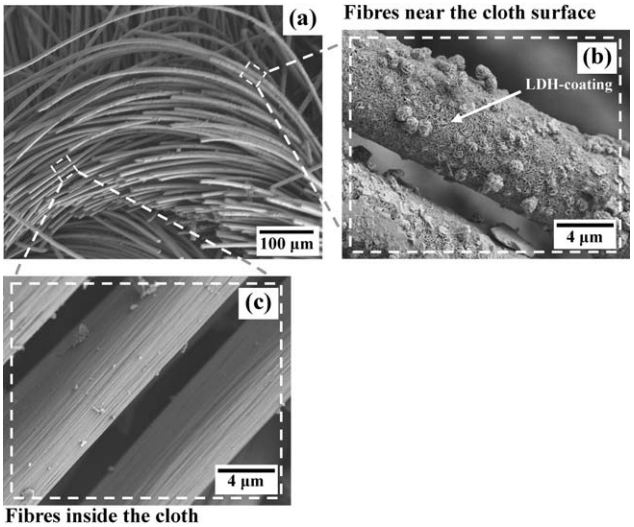

Fig. 15 (a) A side view from the LDH-coated hydrophilic cloth; (b) high magnification of the fibres near cloth's surface, showing LDH coating on surface; (c) high magnification of the fibres inside the cloth, no LDH coatings on them.

rapidly forming highly-oriented Li–Al LDH films on various inert substrates in a metal salt-free system. The metal salt-free method may be extended to rapidly fabricate various LDH ($[Li^{+}_{1-x}M^{3+}_{x}(OH)_2]^{(2x-1)+}$ $[CO^{2-}_3]_{(2x-1)/2}\cdot nH_2O$) thin films. It could be performed on various substrates by immersing them in an Li^{+}- and M^{3+}-containing aqueous solution. Experimentally, the solution was obtained by adding powdered $Li^{+}M^{3+}$ intermetallic compound to a water bath with stirring.

Acknowledgements

Founding for this study came in part from the Ministry of Education grant (Republic of China, Taiwan) under the ATU plan. This work was also financially supported by the National Science Council of Taiwan (Contract No. NSC 98-2221-E-005-028). The authors are grateful for their support.

References

1 F. Cavani, F. Trifiro and A. Vaccari, *Catal. Today*, 1991, **11**, 173–301.
2 C. J. Serna, J. L. Rendon and J. E. Iglesias, *Clays Clay Miner.*, 1982, **30**, 180–184.
3 P. K. Dutta and M. Puri, *J. Phys. Chem.*, 1989, **93**, 376–381.
4 A. V. Besserguenev, A. M. Fogg, R. J. Francis, S. J. Price, D. O'Hare, V. P. Isupov and B. P. Tolochko, *Chem. Mater.*, 1997, **9**, 241–247.
5 S. L. Wang, R. J. Hseu, R. R. Chang, P. N. Chiang, J. H. Chen and Y. M. Tzou, *Colloids Surf., A*, 2006, **277**, 8–14.
6 I. Sissoko, E. T. Iyagba, R. Sahai and P. Biloen, *J. Solid State Chem.*, 1985, **60**, 283–288.
7 M. C. Lin, F. T. Chang and J. Y. Uan, *J. Mater. Chem.*, 2010, **20**, 6524–6530.
8 S. Bhattacharjee, T. J. Dines and J. A. Anderson, *J. Phys. Chem. C*, 2008, **112**, 14124–14130.
9 D. Francova, N. Tanchoux, C. Gerardin, P. Trens, F. Prinetto, G. Ghiotti, D. Tichit and B. Coq, *Microporous Mesoporous Mater.*, 2007, **99**, 118–125.
10 Y. Liu, K. Murata, T. Hanaoka, M. Inaba and K. Sakanishi, *J. Catal.*, 2007, **248**, 277–287.
11 B. Sels, D. De Vos, M. Buntinx, F. Pierard, A. Kirsch-De Mesmaeker and P. Jacobs, *Nature*, 1999, **400**, 855–857.
12 K. Tomohito, S. Shingo and U. Yoshiaki, *Sep. Purif. Technol.*, 2005, **47**, 20–26.
13 P. C. Pavan, G. A. Gomes and J. B. Valim, *Microporous Mesoporous Mater.*, 1998, **21**, 659–665.
14 Y. Wang and H. Gao, *J. Colloid Interface Sci.*, 2006, **301**, 19–26.
15 D. L. Bish, *Bull. Mineral*, 1980, **103**, 170–175.
16 M. Darder, M. Lopez-Blanco, P. Aranda, F. Leroux and E. Ruiz-Hitzky, *Chem. Mater.*, 2005, **17**, 1969–1977.
17 C. Forano, S. Vial and C. Mousty, *Curr. Nanosci.*, 2006, **2**, 284–294.
18 J. H. Choy, S. J. Choi, J. M. Oh and T. Park, *Appl. Clay Sci.*, 2007, **36**, 122–132.
19 A. Corma, S. B. A. Hamid, S. Iborra and A. Velty, *J. Catal.*, 2005, **234**, 340–347.
20 M. B. J. Roeffaers, B. F. Sels, H. Uji-i, F. C. De Schryver, P. A. Jacobs, D. E. De Vos and J. Hofkens, *Nature*, 2006, **439**, 572–575.
21 J. L. Shumaker, C. Crofcheck, S. A. Tackett, E. Santillan-Jimenez and M. Crocker, *Catal. Lett.*, 2007, **115**, 56–61.
22 J. L. Shumaker, C. Crofcheck, S. A. Tackett, E. Santillan-Jimenez, T. Morgan, Y. Ji, M. Crocker and T. J. Toops, *Appl. Catal., B*, 2008, **82**, 120–130.
23 Y. Wang, F. Zhang, S. Xu, X. Wang, D. G. Evans and X. Duan, *Ind. Eng. Chem. Res.*, 2008, **47**, 5746–5750.
24 G. Centi and S. Perathoner, *Catal. Today*, 2003, **79–80**, 3–13.
25 J. Aumo, S. Oksanen, J. P. Mikkola, T. Salmi and D. Y. Murzin, *Ind. Eng. Chem. Res.*, 2005, **44**, 5285–5290.
26 A. Sirijaruphan, J. G. Goodwin Jr., R. W. Rice, D. Wei, K. R. Butcher, G. W. Roberts and J. J. Spivey, *Appl. Catal., A*, 2005, **281**, 1–9.
27 Y. Matatov-Meytal, V. Barelko, I. Yuranov and M. Sheintuch, *Appl. Catal., B*, 2000, **27**, 127–135.
28 B. Louis, P. Reuse, L. Kiwi-Minsker and A. Renken, *Appl. Catal., A*, 2001, **210**, 103–109.
29 Y. Matatov-Meytal, V. Barelko, I. Yuranov, L. Kiwi-Minsker, A. Renken and M. Sheintuch, *Appl. Catal., B*, 2001, **31**, 233–240.
30 T. Boger, M. M. P. Zieverink, M. T. Kreutzer, F. Kapteijn, J. A. Moulijn and W. P. Addiego, *Ind. Eng. Chem. Res.*, 2004, **43**, 2337–2344.
31 M. Uzunov-Bujnova, R. Todorovska, M. Milanova, R. Kralchevska and D. Todorovsky, *Appl. Surf. Sci.*, 2009, **256**, 830–837.
32 J. Sun, X. Wang, J. Sun, R. Sun, S. Sun and L. Qiao, *J. Mol. Catal. A: Chem.*, 2006, **260**, 241–246.
33 Y. Liang, H. B. Dai, L. P. Ma, P. Wang and H. M. Cheng, *Int. J. Hydrogen Energy*, 2010, **35**, 3023–3028.
34 J. L. Williams, *Catal. Today*, 2001, **69**, 3–9.
35 V. Meille, *Appl. Catal., A*, 2006, **315**, 1–17.
36 L. Zhao, D. Yang, M. Dong, T. Xu, Y. Jin, S. Xu, F. Zhang, D. G. Evans and X. Jiang, *Ind. Eng. Chem. Res.*, 2010, **49**, 5610–5615.
37 X. Guo, F. Zhang, D. G. Evans and X. Duan, *Chem. Commun.*, 2010, **46**, 5197–5210.
38 J. Y. Uan, J. K. Lin and Y. S. Tung, *J. Mater. Chem.*, 2010, **20**, 761–766.
39 Y. Du, G. Hu and D. O'Hare, *J. Mater. Chem.*, 2009, **19**, 1160–1165.
40 L. Li, R. Ma, Y. Ebina, N. Iyi and T. Sasaki, *Chem. Mater.*, 2005, **17**, 4386–4391.
41 J. H. Lee, S. W. Rhee and D. Y. Jung, *J. Am. Chem. Soc.*, 2007, **129**, 3522–3523.
42 K. Okamoto, T. Sasaki, T. Fujita and N. Iyi, *J. Mater. Chem.*, 2006, **16**, 1608–1616.
43 Z. Lu, F. Zhang, X. Lei, L. Yang, S. Xu and X. Duan, *Chem. Eng. Sci.*, 2008, **63**, 4055–4062.
44 H. Chen, F. Zhang, T. Chen, S. Xu, D. G. Evans and X. Duan, *Chem. Eng. Sci.*, 2009, **64**, 2617–2622.
45 J. Liu, X. Huang, Y. Li, K. M. Sulieman, X. He and F. Sun, *J. Phys. Chem. B*, 2006, **110**, 21865–21872.
46 J. Liu, Y. Li, X. Huang, G. Li and Z. Li, *Adv. Funct. Mater.*, 2008, **18**, 1448–1458.
47 X. Guo, F. Zhang, S. Xu, Z. Cui, D. G. Evans and X. Duan, *Ind. Eng. Chem. Res.*, 2009, **48**, 10864–10869.
48 Z. Lu, F. Zhang, X. Lei, L. Yang, D. G. Evans and X. Duan, *Chem. Eng. Sci.*, 2007, **62**, 6069–6075.
49 X. Guo, F. Zhang, S. Xu, D. G. Evans and X. Duan, *Chem. Commun.*, 2009, 6836–6838.
50 Y. Zhao, S. He, M. Wei, D. G. Evans and X. Duan, *Chem. Commun.*, 2010, **46**, 3031–3033.
51 X. Li, J. Liu, X. Ji, J. Jiang, R. Ding, Y. Hu, A. Hu and X. Huang, *Sens. Actuators, B*, 2010, **147**, 241–247.

52 L. Indira and P. Vishnu Kamath, *J. Mater. Chem.*, 1994, **4**, 1487–1490.
53 E. Scavetta, A. Mignani, D. Prandstraller and D. Tonelli, *Chem. Mater.*, 2007, **19**, 4523–4529.
54 M. S. Yarger, E. M. P. Steinmiller and K. S. Choi, *Inorg. Chem.*, 2008, **47**, 5859–5965.
55 J. K. Lin, C. L. Hsia and J. Y. Uan, *Scr. Mater.*, 2007, **56**, 927–930.
56 J. K. Lin and J. Y. Uan, *Corros. Sci.*, 2009, **51**, 1181–1188.
57 C. A. Drewien, M. O. Eatough, D. R. Tallant, C. R. Hills and R. G. Buchheit, *J. Mater. Res.*, 1996, **11**, 1507–1513.
58 C. J. Serna, J. L. White and S. L. Hem, *Clays Clay Miner.*, 1977, **25**, 384–391.
59 I. C. Chisem and W. Jones, *J. Mater. Chem.*, 1994, **4**, 1737–1744.
60 D. Li, Z. Tuo, D. G. Evans and X. Duan, *J. Solid State Chem.*, 2006, **179**, 3114–3120.
61 Q. He, S. Yin and T. Sato, *J. Phys. Chem. Solids*, 2004, **65**, 395–402.
62 L. Perioli, V. Ambrogi, B. Bertini, M. Ricci, M. Nocchetti, L. Latterini and C. Rossi, *Eur. J. Pharm. Biopharm.*, 2006, **62**, 185–193.
63 U. Costantino, V. Ambrogi, M. Nocchetti and L. Perioli, *Microporous Mesoporous Mater.*, 2008, **107**, 149–160.